



**International Journal of Sciences:
Basic and Applied Research
(IJSBAR)**

**ISSN 2307-4531
(Print & Online)**

<http://gssrr.org/index.php?journal=JournalOfBasicAndApplied>



**A Study on Amorphous Silicon Electronic Portal Imaging
Device (A-Si EPID) Response to Delivered Radiation
Doses**

Mark Pokoo-Aikins^{a*}, Augustine K. Kyere^b, Moses J. Eghan^c, Samuel N. Tagoe^d, Philip O. Kyeremeh^e, George F. Acquah^f, Francis Hasford^g

^a*Radiological and Medical Sciences Research Institute, Ghana Atomic Energy Commission, P.O Box LG 80, Legon Accra, Ghana*

^b*Department of Physics of the School of Physical Sciences, College of Agriculture and Natural Sciences University of Cape Coast*

^{e,f}*SGMC Cancer Centre, Radiation Oncology Physics, P.O. Box CT 3286, Cantonments Accra, Ghana*

^{b,g}*Graduate School of Nuclear and Allied Sciences, University of Ghana, Department of Medical Physics, P.O. Box AE 1, Atomic, Accra-Ghana*

^d*National Centre for Radiotherapy and Nuclear Medicine Dept., Korle-Bu Teaching Hospital, Ghana*

^a*Email: m.pokoo-aikins@gaecgh.org*

^b*Email: kwaamkyere@gmail.com*

^c*Email: meghan@ucc.edu.gh*

Abstract

The use of amorphous silicon flat panel-type electronic portal imaging device (a-Si EPID) as dosimeters in radiotherapy has seen gradual increase in recent times. This research study has assessed dosimetric response of a-Si EPID (Elekta iViewGT) with respect to photon beam qualities on Elekta Synergy Platform linac. Images acquired under reference conditions of 10×10 cm² open field with the a-Si EPID at source to EPID distance (SED) of 159 cm and varying dose of 1-3 Gy in polymethyl methacrylate (PMMA) solid water phantom slabs were used. The experiment was repeated with Farmer-type PTW ionization chamber (IBA 30010) in position and measurement taken at 10 cm in the solid water phantom .

* Corresponding author.

Set up conditions for EPID and IC remained same throughout the study. The study observed similar and proportional increases in EPID and IC signals with increasing dose. Maximum deviation of 7.2 % was recorded between EPID and IC measurements. Outcome of the study demonstrates that the a-Si EPID is appropriate for dosimetric verification purposes on the Elekta linac. Comprehensive evaluation of dosimetric properties of EPIDs is thus necessary to ensure reliability in dose measurements on different linac systems.

Keywords: Electronic Portal Imaging Devices (EPID); dosimetric properties; radiation dosimetry.

1. Introduction

In radiotherapy, the major challenge of cancer treatment is to destroy the cancerous tumour with the appropriate dose, while the normal surrounding tissues receive the correct radiation dose prescribed in the treatment plan [1-4]. As radiotherapy treatments are becoming more complex with new techniques, the importance of verifying exact delivered doses to patients during external beam cancer treatments has increased. In recent times, the use of electronic portal Devices (EPIDs) has been recognized as a promising technique for radiation dose verifications during radiotherapy procedures[4-6]. It is possible to determine real-time radiotherapy doses to patients using portal images obtained with an EPID, for comparison with the intended planned doses generated from the treatment planning system. It is therefore necessarily important to investigate dosimetric properties of EPID [5-7]. In recent years, electronic portal imaging device (EPID) which was originally developed for the purposes of positional verification of patient setups, has emerged as a promising tool for verifying actual delivered doses to patients during external beam radiation treatments (EBRT). In this study, response of a-Si EPID to delivered doses in EBRT is evaluated for its effectiveness in verification of doses .

2. Materials and Methods

2.1. Materials

Materials employed in the study include Elekta Synergy Platform linear accelerator (linac) equipped with electronic portal imaging device at the SGMC Cancer Centre, Farmer-type ionization chamber (IBA 30010) and slabs of PMMA solid water phantom. The clinical linac produces photon beams of energies 6 and 15 MV, and electron beams of energies 6, 10 and 15 MeV. For this study, only the 15 MV photon beam was used, and all irradiations were done at 0° gantry angle and 0° collimator position. The a-Si EPID was mounted on robotic arm at source to EPID distance (SED) of 159 cm and comprises an image detector unit with an active MV detector area of 41×41 cm² (approximately 26×26 cm² at isocentre) and resolution of 1024×1024 16-bit pixels images acquired by iViewGTTM Elekta software (version R3.02). The iViewGT™ provides 2-dimensional megavoltage planar images within a fraction of a second, and helps in achieving excellent clearance and superior field of view [8]. Additionally, the iViewGT™ automatically applies a set of corrections to all images measured, including offset and gain correction as well as a bad pixel map correction. In acquiring EPID images in iViewGT™, pixel values are automatically re-normalized before saving the image data to the database[8]. The slabs of PMMA phantom (PTW Freiberg) have dimensions of 30×30 cm², designed for range of 70 kV to 50 MV photon energies and 1 MeV to 50 MeV electron energies [9]. Each slab has a

thickness of 1 cm .



Figure 1: Pack of 30×30 cm² PMMA phantom slabs used in this study.

2.2. Methods

In the study, the relation between delivered doses and EPID signal (represented by greyscale pixel values) was investigated using clinically applicable range of doses at the SGMC Cancer Centre. Computed tomography image was taken for specific localization of the PMMA phantom and treatment plans were generated using Ocentra Masterplan treatment planning system (TPS). The phantom was then treated in accordance with the treatment plan. The plan was optimized for 6 MV photon beam energy, and all irradiations in the treatment room were done with photon energy of 6 MV. Figure 2 is schematic diagram of the experimental treatment setup .

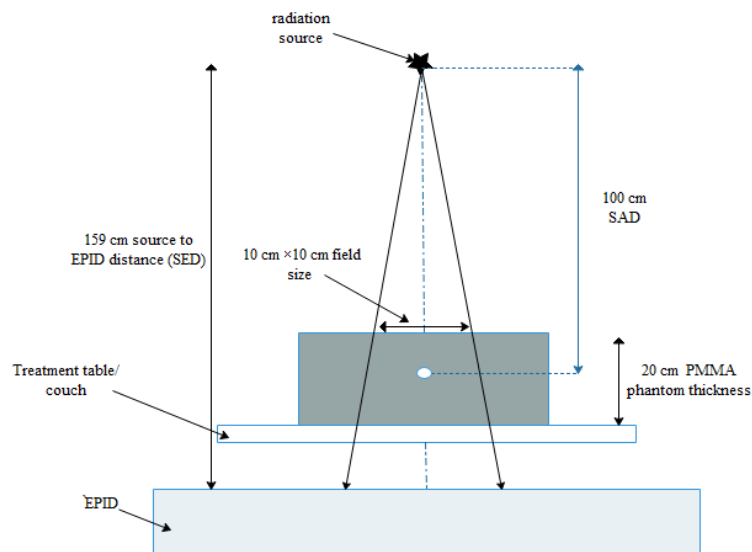


Figure 2: A schematic diagram of the experimental setup for measurements

During acquisition of images on the EPID system, each image was assigned a unique pixel scaling factor (PSF) saved in the database. The originally accumulated pixel value corresponding to the original EPID signal (S_{EPID}) is determined by dividing the recorded pixel value by the PSF as shown in Equation 1 .

$$S_{EPID} = \frac{\text{Recorded pixel value}}{\text{Pixel Scaling Factor (PSF)}} \quad (1)$$

All EPID measurements were obtained at the isocentre of the beam through irradiation of 20 cm thickness of the PMMA solid water phantom with delivered doses ranging from 1-3 Gy for 10 × 10 cm² field size at 159 cm source to EPID distance (SED), and an isocentre depth of 10 cm. A 100 cm source to axis distance (SAD) technique was employed in all irradiations. All images obtained were exported into Image J software, and the mean grayscale pixel values within 10 × 10 mm² region of interest (ROI) at the centre of the field were measured and a graph of mean grayscale pixel value was plotted against delivered dose using Minitab statistical tool (version 18.1). The experiment was repeated with Farmer-Type ionization chamber (IBA 30010) and measurements taken at depth of 10 cm in the PMMA phantom. Experimental set ups for both EPID and IC measurements were kept the same. The effective point of measurement was at the isocentre of at 10 cm depth in the PMMA phantom .

3. Results and discussion

3.1. Dose Linearity response with EPID Signal (S_{EPID})

Table 1 shows the results of ion chamber (IC) measurements and EPID signal readings obtained for dose response to EPID. Each IC measurement had been repeated twice, and the results averaged and corrected for temperature and pressure. In this table, EPID signal readings (grayscale pixel values) and the corrected averaged IC values (in Gy) are provided for their corresponding delivered doses. The EPID and IC data were normalized to dose value of 1 Gy . In Figure 3, a graphical representation of EPID signal dependence on dose, indicated by a red fitted line is shown. It was observed that measurements for EPID signal values (grayscale pixel values) showed strong positive correlation with varying range of doses from 1 - 3 Gy. The degree of linearity was observed to be high, and further observances showed that for every change in the mean pixel value of the EPID signal, the fitted line rises or falls by 0.000001 Gy. The increase in EPID signal response as a result of increment in delivered radiation dose, can be attributed to variations in attenuation of primary photon beams through the phantom. The higher the delivered radiation dose to the phantom (higher MU), more radiation is likely to reach the EPID sensitivity area due to lesser attenuation of primary photon beams of higher energies, and also as result of increase in radiation scatter reaching the EPID sensitivity area. This EPID Signal – Dose response linearity agrees with those that were obtained by Wendling and his colleagues [5] and Dina and his colleagues [10]. In their work, Wendling et. al attributed these variations in EPID response to varying dose to contribution of scatter within the EPID, the contribution of scatter within the phantom, the contribution of scatter resulting from the phantom to the EPID and the attenuation of the primary photon beams through the phantom. Therefore, the mean greyscale EPID pixel value was highly dependent on radiation dose delivered . Additionally, the higher

linear value of coefficient of determination R-Sq (99.6 %) shown in Figure 3 indicates that 99.6% of the variance in dose is accounted by EPID signal grayscale pixel values. Moreover, the dataplots are all within 95% confidence interval, and hence there is 99% confidence that the true mean is contained in the interval, thereby indicating higher precision. Hence the fitted line truly describes the trend in the data, and EPID can be considered appropriate for measuring patient absorbed doses for radiotherapy daily quality assurances .

Table 1: Results of the EPID Signal and Ionization chamber analysis for varying radiation doses

Delivered Dose (Gy)	Raw EPID Signal (Greyscale pixel value)	PSF	Original Accumulated pixel value (S_{EPID})	Normalized EPID Signal ($S_{EPID_normalized}$)	Averaged Ion Chamber Reading (nC)	Normalized IC values	% deviation between Normalized IC values and Normalized EPID Signal values
1.0	26218.542	0.024930	1051648.257	1.000	18.06	1.000	0.0%
1.1	26236.871	0.020670	1269321.287	1.207	20.45	1.133	6.5%
1.2	26294.245	0.019822	1326534.125	1.261	22.04	1.221	3.3%
1.3	26232.666	0.018390	1426463.622	1.356	22.95	1.271	6.7%
1.4	26240.758	0.016550	1585544.290	1.508	25.51	1.413	6.7%
1.5	26265.524	0.016292	1612156.248	1.533	27.09	1.500	2.2%
1.6	26225.040	0.015050	1742527.575	1.657	28.05	1.553	6.7%
1.7	26229.662	0.013780	1903458.781	1.810	30.61	1.695	6.8%
1.8	26240.053	0.012700	2066145.906	1.965	33.12	1.834	7.1%
1.9	26243.125	0.012524	2095423.246	1.993	35.21	1.950	2.2%
2.0	26238.998	0.011750	2233106.213	2.123	35.78	1.982	7.1%
2.1	26235.384	0.010960	2393739.416	2.276	38.35	2.124	7.2%
2.2	26264.453	0.010915	2406240.125	2.288	39.74	2.201	4.0%
2.3	26283.124	0.010363	2536321.524	2.412	41.55	2.301	4.8%
2.4	26292.451	0.010011	2626423.124	2.497	43.35	2.401	4.0%
2.5	26245.351	0.009626	2726432.214	2.593	45.16	2.501	3.7%
2.6	26261.215	0.009338	2812325.241	2.674	46.97	2.601	2.8%
2.7	26266.214	0.008918	2945212.718	2.801	48.77	2.701	3.7%
2.8	26279.894	0.008520	3084324.214	2.933	50.58	2.801	4.7%
2.9	26265.234	0.008377	3135466.215	2.981	52.39	2.901	2.8%
3.0	26281.569	0.008099	3245231.234	3.086	54.26	3.005	2.7%

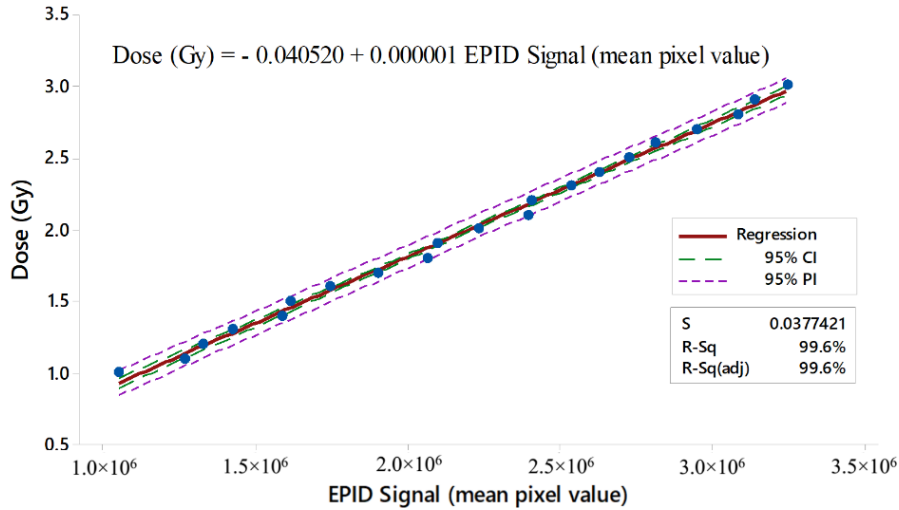


Figure 3: The graphical representation of EPID Signal response to varying delivered doses.

Additionally, the hypothetical output for the regression in Figure 3 is shown in Table 1. It is seen that the p-value (<0.005) is much less than the significance level of 0.05. The null hypothesis of normality is therefore rejected, and conclusion is drawn that there is a statistically significant difference among the population means. The test statistics is therefore significant at the 5% level. This is further explained by the residual plots provided for dose (Figure 4)

Table 2: Hypothetical output for the regression from Dose-EPID Signal plots.

Term	Coef	SE Coef	T-Value	P-Value	VIF
Constant	-0.040500	0.029000	-1.40	0.178	-
EPID Signal (mean pixel value)	0.000001	0.000000	73.39	0.000	1.00

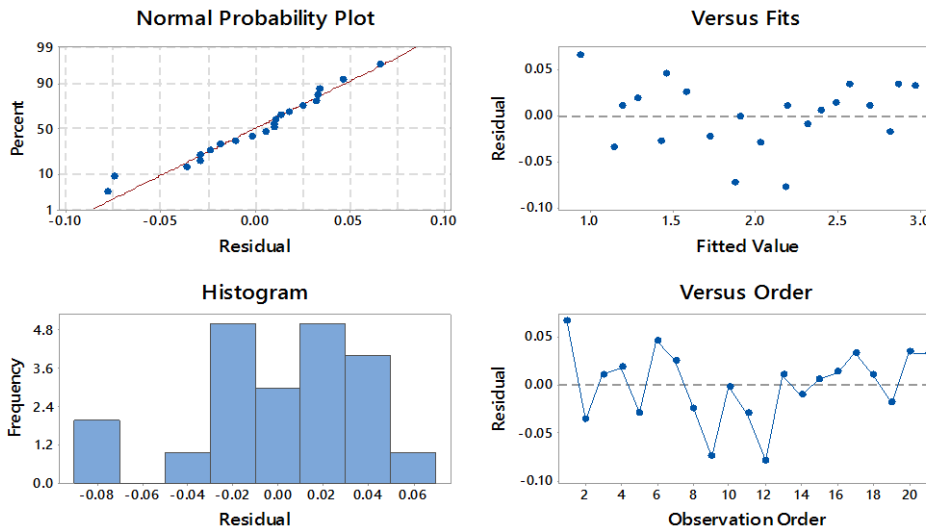


Figure 4: The graphical representations of various residual plots for delivered radiation doses.

In Figure 4, the residual plots of absorbed dose is presented. The points on the normal probability plot form a nearly linear pattern, which indicates that the normal distribution is a good model for this data set. Additionally, the scatter plot of residuals versus fitted values demonstrates a random pattern. The residuals fall randomly around the fitted values, indicating a linear relationship between EPID Signals and absorbed dose. Likewise, the residual versus order plot suggests that there is a positive serial correlation among the error terms, and that a strong positive correlation is observed. Moreover, the histogram residual plot shows the frequency of residual values, with two peaks at -0.02 and 0.02 respectively, and indicating non-symmetric properties, and hence being bimodal in nature. The histogram plots is centred at 0.00, and further provides a range from -0.08 to 0.06, with a gap at -0.6 without any outliers, entailing that the model meets all the assumptions of linear regression .

$$D(\text{Gy}) = -0.040520 + (1 \times 10^{-6} \times S_{EPID}) \quad (2)$$

In equation 2, the regression equation resulting from the plot of delivered dose as a function of EPID Signal (original accumulate pixel value) is provided. The equation shows that the coefficient for EPID signal in pixel values is 0.000001 Gy. This coefficient indicates that for every additional pixel value of EPID signal, the dose is expected to increase by an average of 0.000001 Gy .

3.2. Varying Doses: EPID versus Ionization Chamber (IC)

Comparisons between EPID and IC scatter plots at delivered doses of 1 - 3 Gy are presented in Figure 5. The figure portrays the plots of normalized values of EPID Signal and their corresponding Ionization chamber readings. Comparatively, results from the EPID measurements and the ionization chamber (IC) measurements show identical response to varying doses (Figure 5), a maximum and minimum deviations recorded as 7.2 % and 0.0 % respectively (as shown in Table 1). The gradient of the EPID measurements does not vary greatly from that for the ion chamber measurements. The ionization chamber used in this comparison is used for absolute measurements of the linear accelerator output. This means that the EPID is comparable and traceable to the ionization chamber which is well calibrated and known to have a high accuracy in detecting deviations in linac output. The test therefore proves that the EPID data points have a strong correlation with dose within this range, and that the gradient is adequate to resolve discrepancies in linac output.

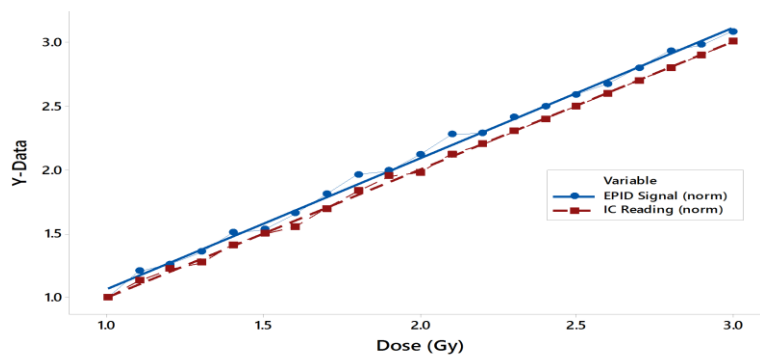


Figure 5: The graphical representation of comparisons between EPID and IC scatter plots at same delivered doses.

4. Conclusion

The accuracy of electronic portal imaging devices as a tool for radiotherapy dosimetric purposes has been highlighted in this study. The comparability of a-Si EPID (Elekta iViewGT) to Farmer-type ionization chamber in the study is an indication that the a-Si EPID can be used for dosimetric purposes, especially in cases of verifying doses to patients undergoing external beam radiotherapy (EBRT).

References

- [1]. Y. Lemoigne and A. Caner, *Radiotherapy and Brachytherapy*, no. 1. 2007.
- [2]. IAEA, *Development of procedures for in vivo dosimetry in radiotherapy*. IAEA Human Health Reports No. 8, IAEA Human. 2013.
- [3]. A. Barrett, J. Dobbs, S. Morris, and T. Roques, *Practical radiotherapy planning*, 4th Editio. Hodder Arnold company, 2009.
- [4]. S. Nijsten, "Portal Dosimetry in Radiotherapy," 2009.
- [5]. M. Wendling, R. J. W. Louwe, L. N. McDermott, J. J. Sonke, M. Van Herk, and B. J. Mijnheer, "Accurate two-dimensional IMRT verification using a back-projection EPID dosimetry method," *Med. Phys.*, vol. 33, no. 2, pp. 259–273, Jan. 2006.
- [6]. K. Slosarek, M. Szlag, B. Bekman, and A. Grzadziel, "EPID in vivo dosimetry in RapidArc technique," *Reports Pract. Oncol. Radiother.*, vol. 15, no. 1, pp. 8–14, 2010.
- [7]. B. L. Seng, "2-D Dose Measurement Using a Flat Panel Epid," University of British Columbia, 2008.
- [8]. Elekta, "iViewGTTM R3.02 - R3.4 Manual," 2010.
- [9]. PTW, "User Manual Farmer Chamber Ionization Chamber," pp. 1–42, 2016.
- [10]. N. E. S. Dina Abdelaziz, Wafaa Khalifa, "Efficacy of Use of A-Si EPID as Imaging Device in IMRT QA," *IOSR J. Appl. Phys.*, vol. 7, no. 1, pp. 27–43, 2015.